JGR Earth Surface

RESEARCH ARTICLE
10.1029/2018JF004945

Stability Conditions of Peat Plateaus and Palsas in Northern Norway

L. C. P. Martin[1], J. Nitzbon[2], K. S. Aas[1], B. Etzelmüller[1], H. Kristiansen[1], and S. Westermann[1]

[1]Department of Geosciences, University of Oslo, Oslo, Norway, [2]Alfred Wegener Institute, Potsdam, Germany

Key Points:
- We investigate the role of soil water balance and snow depth in permafrost peat plateau stability
- We present a data set gathering distributed measurements of driving parameters for a statistically robust number of observations
- We couple this data set to soil thermal modeling to provide significant results on peat plateau stability conditions

Supporting Information:
- Data S1
- Table S1
- Data Set S1

Correspondence to:
L. C. P. Martin,
leo.doug.martin@gmail.com

Citation:
Martin, L. C. P., Nitzbon, J., Aas, K. S., Etzelmüller, B., Kristiansen, H., & Westermann, S. (2019). Stability conditions of peat plateaus and palsas in northern Norway. *Journal of Geophysical Research: Earth Surface*, *124*, 705–719. https://doi.org/10.1029/2018JF004945

Received 8 NOV 2018
Accepted 6 FEB 2019
Accepted article online 12 FEB 2019
Published online 2 MAR 2019

©2019. American Geophysical Union. All Rights Reserved.

Abstract Peat plateaus and palsas are characteristic morphologies of sporadic permafrost, and the transition from permafrost to permafrost-free ground typically occurs on spatial scales of meters. They are particularly vulnerable to climate change and are currently degrading in Fennoscandia. Here we present a spatially distributed data set of ground surface temperatures for two peat plateau sites in northern Norway for the year 2015–2016. Based on these data and thermal modeling, we investigate how the snow depth and water balance modulate the climate signal in the ground. We find that mean annual ground surface temperatures are centered around 2 to 2.5 °C for stable permafrost locations and 3.5 to 4.5 °C for permafrost-free locations. The surface freezing degree days are characterized by a noticeable threshold around 200 °C.day, with most permafrost-free locations ranging below this value and most stable permafrost ones above it. Freezing degree day values are well correlated to the March snow cover, although some variability is observed and attributed to the ground moisture level. Indeed, a zero curtain effect is observed on temperature time series for saturated soils during winter, while drained peat plateaus show early freezing surface temperatures. Complementarily, modeling experiments allow identifying a *drainage effect* that can modify 1-m ground temperatures by up to 2 °C between drained and water accumulating simulations for the same snow cover. This effect can set favorable or unfavorable conditions for permafrost stability under the same climate forcing.

1. Introduction

The thawing of permafrost at large spatial scale affects the atmospheric concentration of greenhouse gases (CO_2, CH_4) and the global climate through the decomposition of the organic carbon stored in the soils (Walter et al., 2006). This "permafrost carbon feedback" was identified as one of the drivers of the atmospheric CO_2 concentration during the last deglaciation (Crichton et al., 2016; Köhler et al., 2014). Therefore, quantifying its contribution to global warming for the decades to come is necessary to provide accurate climatic scenarios (Koven et al., 2011, 2015; McCalley et al., 2014; Schuur et al., 2009). Yet important uncertainties remain on the timing and amplitude of this contribution because the impact of climate change on permafrost is indirect and implies several positive and negative local feedback related to the soil properties, the hydrology, the microtopography, and the vegetation (Ciais et al., 2013; Schuur et al., 2013).

The soil moisture and the modification of the local hydrology are key controls of the permafrost degradation in response to climate changes (Liljedahl et al., 2016; Zona, 2016). Soil moisture impacts the latent heat exchange during seasonal freezing/thawing and the soil thermal properties that govern the magnitude of the heat flux in the ground during summer and winter. Drainage conditions and lateral water fluxes are therefore important drivers of the soil response to the temperature warming occurring over the Arctic (Koven et al., 2013) and partly control permafrost stability and its thermal response.

Peatland permafrost covers extensive areas such as the Western Siberian Lowlands (900,000 km^2) where permafrost evolves from north to south from continuous to discontinuous and sporadic. This region stores more than 50×10^6 t of carbon (Kremenetski et al., 2003) and shows first evidence of permafrost disappearance and increase in active layer thickness due to climate change (Romanovsky et al., 2010; Sherstyukov & Sherstyukov, 2015). Therefore, the evolution of the peat plateau and palsas is important for the global permafrost state and areas in which degradation is currently ongoing offer great potential to investigate the processes driving their thermal regime.

Peat plateaus and palsas are permafrost landforms which occur in the sporadic permafrost zone (Seppälä, 1972; Sollid & Sørbel, 1998), typically in areas with mean annual ground temperature around 0 °C and

limited precipitation (<800 mm/year; Aalto et al., 2017; Parviainen & Luoto, 2007). It is thus a warm type of permafrost and its distribution is highly sensitive to climate changes (Aalto et al., 2014, 2017; Fronzek et al., 2010; Luoto et al., 2004). Climate change has already driven the limit of continuous and discontinuous permafrost in the North Hemisphere northward (Thibault & Payette, 2009), and ongoing degradation of peat plateaus, which started at least in the 1950s, is observed in the Canadian Arctic and Fennoscandia (Borge et al., 2016; Jones et al., 2016; Mamet et al., 2017; Payette et al., 2004). Analyzing aerial imagery, Borge et al. (2016) quantified the evolution of the areal extent of four peat plateau sites in Northern Norway (Finnmark) between the 1950s and the 2010s and reported a decrease of their lateral extent between 33 and 71%, with the largest lateral changes during the last decade. These results confirmed the crucial role of lateral erosion in permafrost degradation and the importance of the lateral fluxes (snow, water, and heat) and geometric relationship between the plateaus and surrounding mires in this processes. In order to improve the representation of permafrost degradation processes the land surface models used in the Earth system models, Aas et al. (2019) presents an implementation of the lateral fluxes of snow, water, and heat in the Noah MP land surface model. Based on the coupled modeling of two interacting tiles, this model is used to simulate the degradation of the Northern Norway peat plateaus during the coming century and provide a first-order reproduction of the main related processes such as subsidence and soil moisture modification.

Permafrost formation and thermal stability are highly dependent on the peat bog hydrology and vegetation that enable the accumulation of thick layers of organic soil (Jorgenson et al., 2010). The hydrologic and thermal characteristics of these peat soils are particularly favorable to permafrost. The thermal conductivity of the wet peat is several times higher when the peat is frozen than when it is unfrozen (Kujala et al., 2008; Riseborough, 2002), giving rise to a large thermal offset (mean annual permafrost surface temperature minus mean annual ground surface temperature; Romanovsky & Osterkamp, 1995). The southernmost occurrences of permafrost in the North Hemisphere are restricted to peat plateaus and palsas and the ability of peat to host permafrost led authors to classify these features as *ecosystem-driven permafrost* (Shur & Jorgenson, 2007).

The mean annual ground surface temperature (MAGST) and freezing degrees days (FDD) are important variables that drive the distribution of peat plateaus and palsas (Luoto et al., 2004). Given peat thermal properties, the influence of the summer air temperature (measured by thawing degree days) is less critical, and warmer summers have been reported to have little influence on their stability (Seppälä, 2011). However, the summer precipitation and summer soil moisture modifications have been reported as important parameters controlling the peat plateau dynamics. A wet summer can produce drastic thawing of the palsa ice core (Seppälä, 1982), as well as a flooding (Seppälä, 2011). The insulation effect of the winter snow cover plays a prominent role in ground thermal regime (Jorgenson et al., 2010; Romanovsky & Osterkamp, 1995; Way et al., 2018). The relative top position of the peat plateaus compared to the surrounding mires enables the snow deposited on this morphology to be blown away and maintain a shallow snow cover and thus relatively weaker insulation to winter heat losses (Payette et al., 2004).

Altogether, the fast degradation of Fennoscandian peat plateaus (Borge et al., 2016) has potential as analogue for the future and gives the opportunity for field measurements and process-based approaches to further understand the local drivers of permafrost peatland dynamics. In this perspective, a quantitative assessment of the impact of the local snow depth and water balance on permafrost stability conditions of peat plateaus is missing. Here we present a monitoring data set of peat plateaus and palsas for two sites of Northern Norway. For a total of 85 locations distributed over these two sites, time series of ground surface temperature were collected over the year 2015–2016, as well as March 2016 snow depth and August 2016 thaw depth. Based on this data set and simulations with the CryoGrid3 permafrost model (Westermann et al., 2016), we investigate the role of the water balance, particularly subsurface water fluxes and their interaction with the snow cover, and quantify their impact on the surficial and deeper ground thermal regime.

2. Study Area

The study focuses on two peat plateau sites in Norway, located in the northernmost county of Finnmark (68–71°N). Finnmark includes a mountainous coastal region bordering the Norwegian and Barents Seas and an interior region, the Finnmarksvidda, bordered by Finland on the south and east. Finnmarksvidda is a

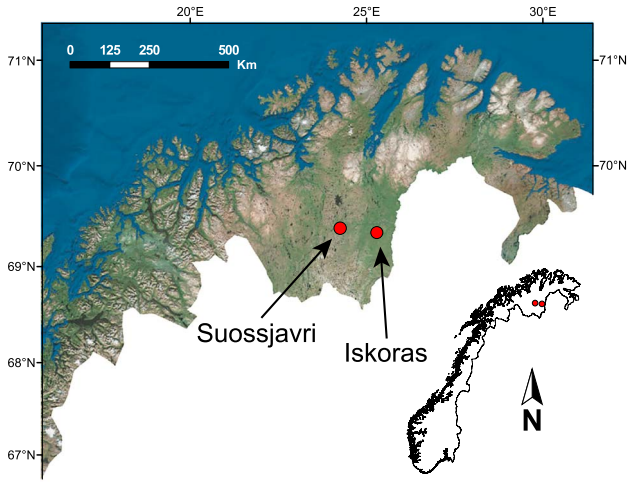

Figure 1. Location of the peat plateau sites of Iskoras (354 m asl) and Suossjavri (310 m asl) in Norway.

plateau area between 300 and 500 m above sea level (asl), with local summits reaching 600 m asl. The region was fully ice-covered during the Pleistocene glaciations and glacial activity shaped the surficial geology with the deposition of ground moraine, glaciofluvial, and glaciolacustrine sediments (Sollid et al., 1973). The climate of Finnmarksvidda is continental with mean annual air temperature between −2 and −4 °C (10 °C for June-July-August, −15 °C for December-January-February (Aune, 1993), for the 1961–1990 period). The mean annual precipitation is less than 400 mm and the mean maximum snow depth lower than 50 cm. The mean annual number of days with dry snow is usually between 150 and 200, and the mean fraction of snow of the total precipitation is usually less than 40% (Borge et al., 2016; snow data from seNorge.no, for the 19961–1990 period).

The Iskoras peat plateau (69.34°N, 25.29°E; Figure 1) is located 90 km south from the coast of the closest fjord. The plateau lies around 350 m asl and covers approximately 4 ha. The Suossjavri peat plateau (69.38°N, 24.25°E; Figure 1) is bordered by the Suossjavri Lake on the east and north and the Iesjoka River on the south. It lies around 310 m asl and extends over approximately 23 ha. Both sites present a complex of degrading and laterally carved peat plateaus, as well as smaller peat mounds, interlaced and surrounded by wet mires and ponds. These peat bodies have a metric to pluri decametric extension with complex horizontal geometries (Figure 2) and rise 0.1 to 3 m above the surrounding wet mires (Figure 2). The tops of the peat plateaus are either covered by lichen crusts, mosses, *Ericaceae* (*Empetrum nigrum*, *Rhododendron groenlandicum*), and cloudberry herbs (*Rubus chamaemorus*) or bare ground (dried peat, common in Iskoras, but less frequent in Suossjavri). The wet fens mainly present sphagnum sedges, cotton grass (*Eriophorum*), mosses, and *Betula* shrubs. The edges of the peat plateaus are often radially carved by drainage gullies of varying lengths. While the interior parts of the peat plateaus appear relatively stable, many edges show advanced signs of degradation and lateral

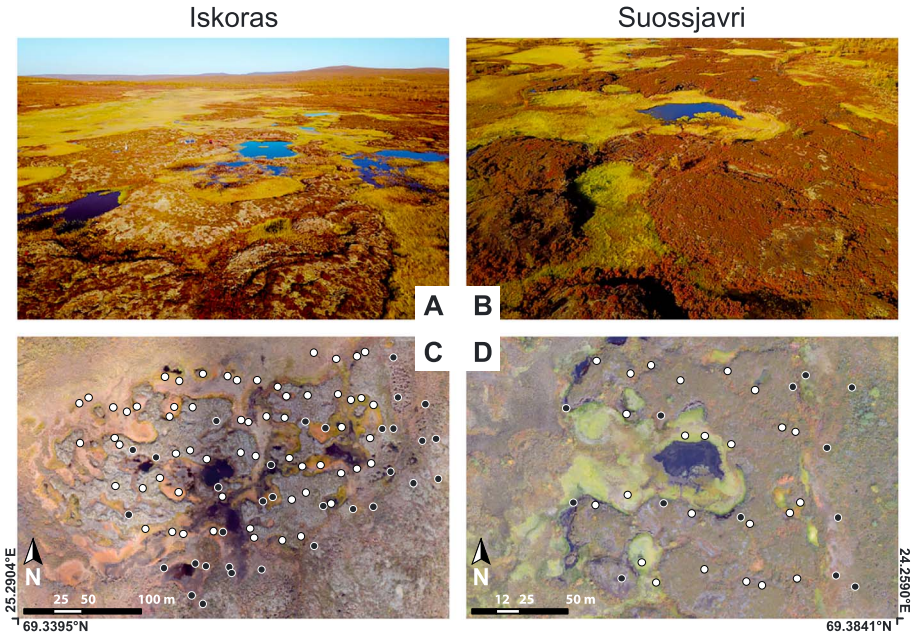

Figure 2. The two sites of Iskoras and Suossjavri. (a and b) Oblique drone photographs of Iskoras and Suossjavri (September 2017). (c and d) Loggers' locations (black and white dots) on drone orthoimages of Iskoras (September 2016) and Suossjavri (September 2015). The loggers were randomly placed inside regularly spaced east-west arrays of grid boxes (not represented here). Results from loggers filled in black are not presented because they are either outside the plateau-palsa-mire complex, have a mineral soil, correspond to a lake/pond, or were dysfunctional.

erosion, with cracks in the peat and tilted peat blocks coming off the plateaus. Depressions also appear on the top of some of the largest plateaus (>10-m diameter) and start forming thermokarst ponds. Based on aerial imagery, Borge et al. (2016) quantified an overall loss of 30% of the Suossjavri peat plateau extent over the last six decades, with a significant acceleration for the last two decades, growing from 0.5%.a^{-1} in the 1960s to 1%.a^{-1} in the 2010s (areal loss rate based on the 1956 extent). They also reported a dimension dependence on the areal degradation rates with the four largest peat plateaus only reducing by 15% of their initial extent over the six decades, whereas smaller peat plateaus and palsas exhibit a 48% decrease. For Iskoras, the same measurements have not yet been performed, but a similar evolution is probable.

For both sites, radiocarbon dating showed that peat development started around 9,800 cal year B.P. in the form of wet fens, which prevailed during most of the Holocene. Evolution of the vegetal macrofossil assemblages shows dry surface conditions associated with permafrost peat plateau aggradation around 950–100 cal year B.P. likely caused by the Little Ice Age cooling (Kjellman et al., 2018).

3. Material and Methods

We rely on measurements of ground surface temperatures and manual probing of thaw depths to test the occurrence of permafrost. We thus have access to a large number of observations (85 loggers in total). A permafrost model tuned to observed parameters, such as snow depth and surface temperature records, is then used to perform sensitivity analysis and focus on deeper subsurface temperatures.

3.1. Field Measurements

3.1.1. Ground Surface Temperature

We designed two networks of more than 100 locations in total, covering the peat plateau and palsa—mire complexes of Iskoras and Suossjavri. These locations were randomly distributed inside regular grid boxes (see Figure 2) to provide a representative distribution of the entire area. Only 61 locations in Iskoras and 24 in Suossjavri were retained for this study (85 loggers in total; white filled dots on Figure 2). The other locations are either located outside the mire complex, correspond to lakes/ponds, have mineral soil, or encountered technical problems with data collection. For each location, we measured the ground surface temperature using iButton® temperature loggers (model DS1922L, accuracy: ±0.5 °C, resolution: 0.5 °C). These loggers were buried between 2 to 5 cm below the uppermost layer of vegetation or soil so that they did not directly receive solar radiation. Loggers on peat plateaus were packed with duct tape and those facing wetter conditions were cased in heat-shrink tubes. These loggers recorded the ground surface temperature every 4 hr without interruption from September 2015 to August 2016.

3.1.2. Snow Depth

For each temperature-logger location, the snow depth was measured in the end of March 2016 with an avalanche probe. The exact location of each logger under the snow cover was localized using a dGPS system to ensure a decimetric accuracy.

3.1.3. Thaw Depth

For each temperature-logger location, the presence of permafrost and the thaw depth was measured in the beginning of September 2016 by manual probing. These depths provide a good estimate of the maximum thaw depth of the year as they are taken at the end of the summer and before the first negative temperatures in October. When no permafrost was detected in the first meter, the location was considered free of near-surface permafrost. When permafrost was detected, the distribution of thaw depths was used to estimate sites with “stable permafrost” and “degrading permafrost” consistently with previous studies (Åkerman & Johansson, 2008; see Figure 4a and section 4.1). In this study, we focus on the difference between stable permafrost and permafrost-free locations. The “stable/instable” classification refers to the subsurface thermal regime and does not include the possible case where permafrost degradation occurs from the bottom, leading to subsidence without affecting the active layers.

3.2. Modeling the Ground Thermal Regime

3.2.1. The CryoGrid3 Model and Modifications

To explore the role of the water fluxes and the snow deposition, on the peat plateau's stability, we use the CryoGrid3 model (CG3; Westermann et al., 2016), a land surface model designed for permafrost modeling. It consists of a physically based description of 1-D heat transfer in the soil column, including freeze–thaw process of soil water/ice. The model features a simple snowpack module which includes

heat conduction, dynamic buildup, melt, sublimation, water infiltration, and refreezing. In the versions demonstrated by Westermann et al. (2016) and Langer et al. (2016), soil water contents are prescribed and considered constant in time which is a major limitation in areas with strongly changing soil moisture conditions. As a consequence, evapotranspiration in the model is governed by a separate parameter, the "surface resistance against evapotranspiration," and does not depend on soil moisture (Westermann et al., 2016). In this study, we modify CG3 to improve the water balance and evapotranspiration scheme as described below. The version of CG3 used in Nitzbon et al. (2018) includes the same modifications.

3.2.1.1. Implementation of a Bucket Scheme for Soil Hydrology

The infiltration is now based on a "bucket scheme" (Chen et al., 1996; Figure S1 in the supporting information) where the water input (precipitation + condensation) during one time step infiltrates at once into the first meters of the soil column, until the water table is reached. As water infiltrates, the water content of the soil cells increases until the field capacity is reached, a threshold value that indicates the maximum amount of water a soil cell can hold before drainage occurs. For simplicity, the infiltration is set to only occur when the uppermost soil cell is snow free and unfrozen.

The bucket scheme distributes water cell by cell, starting from top (the soil surface) to the permafrost table (or the limit depth for infiltration, prescribed by the user, in case of permafrost-free conditions) so that the water input fills the cells to field capacity (Figure S1). If the water contents of the uppermost cells exceed the field capacity, the water is moved downward to the next cell. When the water table is reached and water remains, it is distributed from bottom to top to fill the soil cells to saturation and raise the water table. In case of full saturation of the soil, excess water is considered as runoff. To perform sensitivity tests to drainage conditions (Figures 6 and 7 and associated results), an external flux of water can be added or removed at a constant rate.

3.2.1.2. Modification of the Evapotranspiration Scheme

The potential evapotranspiration is computed from the surface energy balance, using the turbulent flux of latent heat obtained by the Monin-Obukhov approach, as initially described in equation (5) in Westermann et al. (2016) . The potential water loss given by this formula is weighted and distributed along the soil column. First, the water uptake is adjusted to match the water availability. The scheme prescribes a nonlinear decrease of the available water for evapotranspiration as the water content of a cell decreases from field capacity to 0. Then, the water uptake is normalized and distributed vertically so that it decreases exponentially with depth, with two different characteristic lengths for evaporation and transpiration. Finally, the scheme adjusts the proportion of evaporation relatively to transpiration based on an input parameter and derives the distributed water loss.

3.2.2. Climatic Forcing for CryoGrid3

The forcing data for CG3 were obtained by dynamically downscaling ERA Interim reanalysis data (Dee et al., 2011) with the Weather Research and Forecasting model (WRF v.3.8.1; Skamarock & Klemp, 2008). The WRF model was run with two nested domains with 15- and 3-km grid spacings from August 2015 to July 2016 and using 3-hourly output from the nearest grid points in the 3-km domain to generate the forcing data set for CG3. Other model options for WRF follows Aas et al. (2016), with the exception of slightly higher vertical resolution (45 model layers compared to 40) and excluding the CMB glacier module.

The year 2015–2016 has been particularly warm in Finnmark (Figure 3). Both 2015 and 2016 ranged 2–3 °C above the 1961–1990 normal period, with the spring (March-April-May) 2016 standing out, being 3–5 °C warmer than normal. Similarly, the period was particularly wet, with 2015 and 2016 being, respectively, 33 and 50% than the normal period. The simulated period therefore provides a good opportunity to study the response of ground surface temperature to this anomalously warm and wet 12-month period (Grinde et al., 2018; Heiberg et al., 2017; MET reports), with these two factors being favorable to permafrost degradation (section 1).

3.2.3. Input Parameters: Model Tuning to Field Data and Soil Stratigraphy

3.2.3.1. Input Soil Stratigraphy

The soil stratigraphy used in the model is based on analyzed soil samples from Iskoras. In September 2015, we collected one surficial and one 50-cm-deep sample in peat soils as well as one in mineral soil at a 45–50-cm depth. We measured the volumetric content of organic and mineral material in these samples to derive a synthetic profile for the modeling experiments which is consistent with coring observations of Kjellman et al. (2018) at the two sites. It consists of a 3-m-thick peat soil layer with 5% of mineral and 15% of

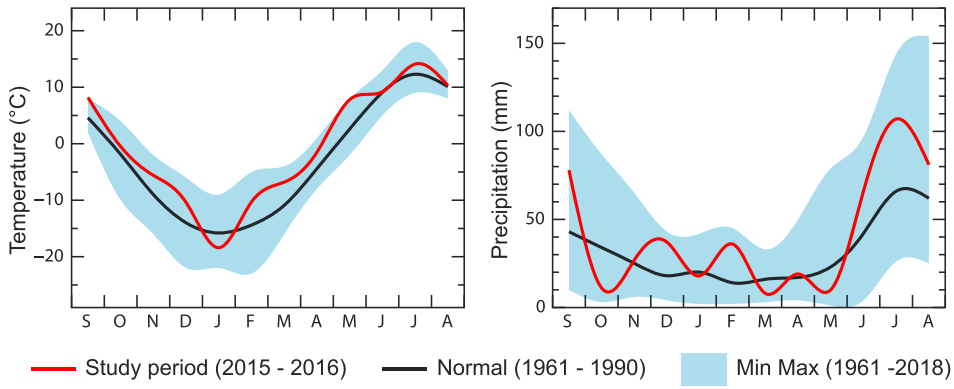

Figure 3. Temperature and precipitation for the study period compared to normal values. Data from the Cuovddatmohkki station (no. 97350) located at 286 m asl, 7 km east from Suossjavri (310 m asl) and 36 km west from Iskoras (350 m asl). Data are from the Norwegian Meteorological Institute (sharki.oslo.dnmi.no).

organic material in total volumetric content (and thus a 80% porosity), underlain by a 7-m saturated mineral silt layer with 50% porosity, above a mineral bedrock layer (3% porosity, as in Westermann et al. (2013)).

3.2.3.2. Field Data and the Snow and Soil Parameters

The field data were used to tune the CG3 model so that it was able to reproduce the surface temperature patterns of the loggers using the forcing data derived from WRF for the same period. Three model parameters were adjusted for this purpose, the field capacity of the soil, the snow density, and the maximum snow depth. The latter is taken as an input threshold for the snowpack buildup above which snow is removed, as in Westermann et al. (2016).

The results of these adjustments can be found in Table S1 in the supporting information. Snow densities of about 230 kg/m^3 produce good results, in line with field measurements we performed in mid-March 2016 in Suossjavri and Iskoras that produced an average snow density of 240 kg/m^3. This is a synthetic value but snow density naturally presents an important variability and has a high impact on the thermal conductivity in the snowpack. The maximum snow depth is highly variable depending on the location, but a snow cover between 20 and 30 cm is common on peat plateaus. Optimal field capacities range from 0.55 to 0.60, which is in line with literature values. Peat soil field capacity can display a pronounced variability (20 to 60% of the volumetric content; Walczak & Rovdan, 2002) and our value is consistent with field observation from Southern Siberian peatlands (Motorin et al., 2017).

3.2.4. Model Setup and Sensitivity Tests

The local snow cover and soil water content are the two main parameters that modulate the climatic signal to create a small-scale ground thermal regime (section 1). To test the ability of CryoGrid3 to reproduce their influence, and further explore permafrost stability conditions, we compared our field data with model outputs using the modified CG3 model with the parameters presented in section 3.2.1.2. The model was forced with a 30-year spin-up of the 2015–2016 climate forcing (section 3.2.1.1) to approximate steady state conditions. With this approach, we observed temperature variations at 1-m depth below 0.02 °C/year. We ran CG3 for various snow depths, covering the range of our observations, and hydrologic configurations as given by the external water flux.

First, we used a negative external flux draining the soil column at a constant rate of 10 mm/day and a positive external flux of water entering the soil column at a constant rate of 10 mm/day. This provided “dry” and “wet” runs from which we calculated the mean annual ground surface temperatures (MAGST). We then compared these runs to the field measurements to evaluate the reliability of the model.

Second, we took advantage of the particularly warm conditions in the study period (section 3.2.1.1), and focus on the 1-m-deep mean annual temperature, to investigate the conditions for thermal sustainability of the peat plateaus. We ran the CG3 model for various values of the snow cover and external water fluxes (inflow and outflow) to explore their ability to allow long-term permafrost stability for such a “warm climate scenario.” We performed runs where the maximum snow depth ranges from 0 to 1 m and for external fluxes of water ranging from −5 to +5 mm/day.

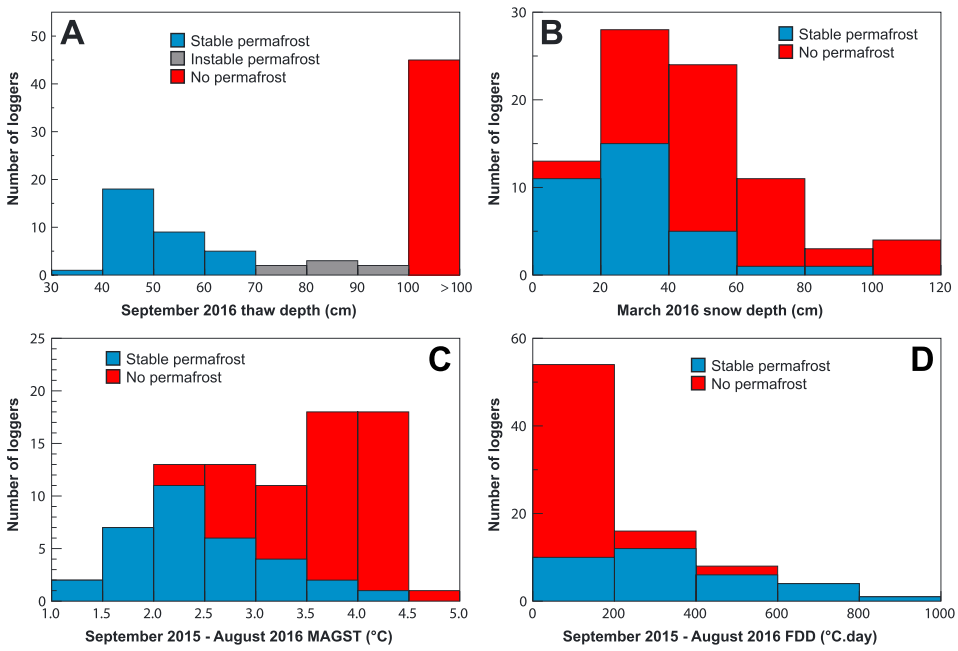

Figure 4. Distribution of the field measurements for the different soil thermal regimes for Iskoras and Suossjavri (merged together). (a) September 2016 thaw depths from which we identify stable permafrost (thaw depth < 65 cm) and instable permafrost (length of the probe is 1 m). (b) March 2016 snow depths. (c) September 2015 to August 2016 mean annual ground surface temperatures. (d) September 2015 to August 2016 freezing degree days. The "stable permafrost" classification refers to the subsurface thermal regime based on active layer measurements and does not include possible subsidence.

4. Results

4.1. Field Measurements

The climatic conditions for the sites of Iskoras and Suossjavri are similar, with mean annual air temperatures from the forcing data differing by 0.13 °C and the annual precipitation by 7%. Based on the loggers, we report an average difference in MAGST between the two sites of 0.5 °C for the stable permafrost locations and of 0.4 °C for the permafrost-free location. The *t* test finds no significant difference between the snow depth data set of Iskoras and Suossjavri (p value = 0.07). For the analysis, we therefore combine the loggers from the two sites in one unique pool, to which modeling results are compared.

4.1.1. Thaw Depths

Field results collected between September 2015 and September 2016 are presented in Figures 4 and 5 and Table 1 (detailed data in Tables S2 and S3 in the supporting information). Figure 4a shows that the September 2016 thaw depths are all larger than 30 cm. When permafrost is present (40 loggers), more than 80% of the values are in the range between 30 and 70 cm and the modal class is the 40–50-cm range. The seven remaining values range between 70 and 100 cm. Based on this distribution, we considered that the main cluster of shallow thaw depths between 30 and 70 cm corresponds to stable permafrost, whereas the sparse and scattered values between 70 and 100 cm indicate degrading permafrost (in agreement with other studies, see section 4.1). As the focus of the paper lies in the comparison of two steady states (presence or absence of permafrost), we did no longer considered these seven locations further in the study. As mentioned before (section 3.1; thaw depths), the use of this "stable/instable permafrost" classification refers to the subsurface thermal regime and does not include the possible case where permafrost degradation occurs from the bottom, leading to subsidence without affecting the active layers.

4.1.2. Snow Depths

The snow depth distribution shows that 70% of the stable permafrost sites are found where the March snow cover is below 30 cm, with a mean value of 27 ± 17 cm (mean ± standard deviation). For permafrost-free locations, more than 80% of the March snow depths are between 20 and 80 cm with a mean value of

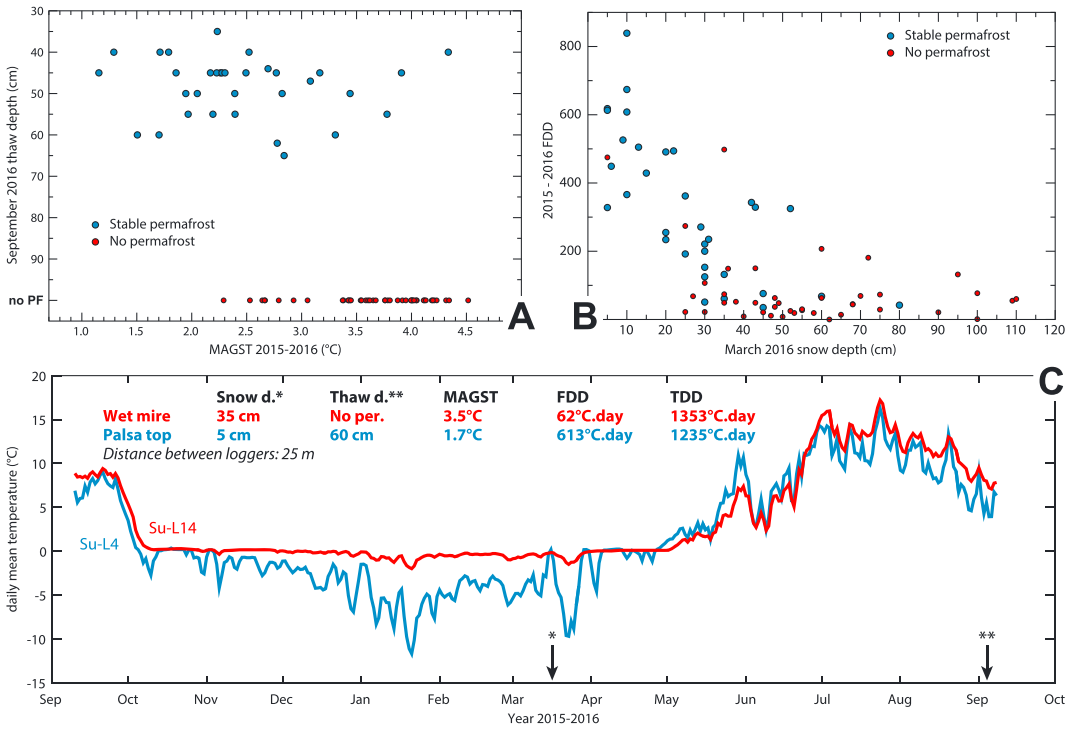

Figure 5. Monitoring data set for Iskoras and Suossjavri (merged together) from September 2015 to September 2016. (a) Mean annual ground surface temperature versus September 2016 thaw depth. (b) March 2016 snow depth versus freezing degree days. (c) Daily mean temperatures recorded by loggers Su-L4 and Su-L14 in Suossjavri and associated field measurements. The asterisk arrows indicate the moment of the year when the snow depth (*) and the thaw depth (**) were measured. See section 3.1 for more details on the measurements and values. The "stable permafrost" classification refers to the subsurface thermal regime based on active layer measurements and does not include possible subsidence.

55 ± 24 cm. The p value from the Student's t test to compare this two populations is inferior to 10^{-4}, yielding highly statistically significant difference between the two populations.

4.1.3. Examples of Temperature Time Series

Examples of temperature times series collected by the loggers are shown in Figure 5c, in which we compare the records of two loggers located 25 m from each other in Suossjavri. Logger 4 is located on top of a peat plateau and Logger 14 in a wet bog at the bottom of this peat plateau. The mid-March snow cover values are low for both loggers, with 5 cm on the plateau top and 35 cm on the wet mire. While no permafrost is observed in August 2016 at the location of Logger 14 (wet mire), Logger 4 (plateau) features a thaw depth of 60 cm (considered stable permafrost). The plateau logger yields a 1.8 °C colder MAGST (1.7 °C compared to 3.5 °C for the plateau logger) than the logger in the wet mire. The daily mean temperatures on the plateau are colder than in the mire 294 days out of 365. The most important difference is during winter with FDD 10 times higher on the plateau.

4.1.4. MAGST

Figure 4C shows the distribution of the MAGSTs. Stable permafrost locations have a mean value of 2.5 ± 0.7 °C and about a third of the values between 2 and 2.5 °C. Permafrost-free locations exhibit

Table 1
Summary of the Field Measurements for the Year 2015–2016

Soil Thermal Status	Indicator	Snow Depth (cm)	Thaw Depth (cm)	MAGST (°C)	FDD (°C.day)
Stable permafrost	Central value	27 ± 17	40–50	2.5 ± 0.7	320 ± 210
	Distribution	70% below 30	Minimum 30	Minimum 2.3	2/3 beyond 200
			Maximum 70	Maximum 4.3	
No permafrost	Central value	55 ± 24		3.7 ± 0.5	80 ± 105
	Distribution	80% between 20 and 80	No active layer	Minimum 2.3	90% below 200
				Maximum 4.5	

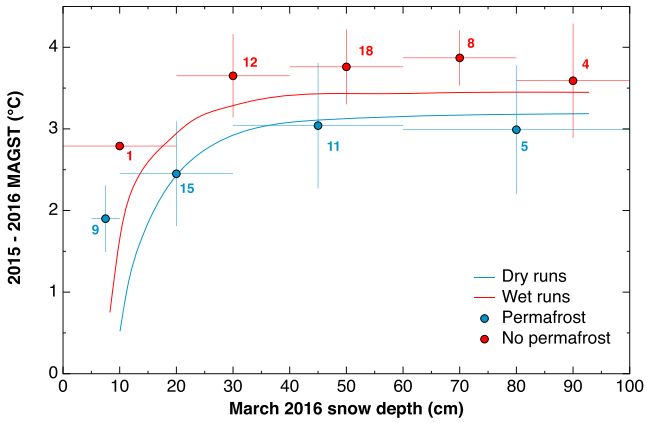

Figure 6. Dependence of the mean annual ground surface temperature (MAGST) on the March snow depth as observed on field data (points) and modeled with CryoGrid3 (lines). Field data: the MAGST are calculated from the temperature time series recorded by loggers located just below the surface. The horizontal bar represents the range of snow depths chosen to calculate the mean. The vertical bar indicates the standard deviations of the MAGSTs inside the snow depth range. The number of loggers is indicated for each point. All loggers with an active layer were included in the "permafrost" category because they all correspond to well-drained conditions. Modeling: the CryoGrid3 model was first tuned to reproduce the local temperature patterns recorded by the loggers and then ran for different snow depths and water input/output. Wet runs correspond to runs receiving 10 mm/day of water and dry runs correspond to runs losing 10 mm/day of water. See methodology for more details. The climatic forcing for these simulations is a spin-up of the 2015–2016 forcing produced with WRF to reach the surface steady state.

MAGSTs ranging from 2.3 to 4.5 °C with a mean value of 3.7 ± 0.5 °C. The p value of the student test is inferior to 10^{-4}, indicating highly statistically significant difference between the two populations. The average MAGST including all logger sites is 3.1 ± 0.8 °C.

Figure 5a shows that the location where the shallowest permafrost table is found does not necessarily correspond to the location where the lowest MAGST is obtained. Stable permafrost is found for a wide range of MAGST, here from 1.2 to 4.3 °C with no particular trend between the MAGST and the thaw depth (r^2 = 0.005).

4.1.5. FDD

The FDD is here taken positive and large values correspond to cold conditions. Two thirds of the stable permafrost locations show values larger than 200 °C.day, with a mean value of 320 ± 210 °C.day. For permafrost-free locations, 90% of the loggers are below 200 °C.day, with a mean value of 80 ± 105 °C.day. Figure 5b highlights the dependence of the ground surface FDD on the snow cover with a rapid decrease of the FDDs with increasing snow depths.

4.2. Comparison of Model Results and Field Temperature Measurements

Figure 6 presents the results of the sensitivity test on snow depth and water balance performed with CG3, compared with field data (see section 3.2.2 for details on methodology). We grouped the field data into different subranges of snow depth for both permafrost and permafrost-free locations, and calculated the mean and standard deviation of the MAGSTs for each subrange.

The figure shows that both the "dry" and "wet" runs (section 3.2.2) can capture the variations of the field-derived MAGST with very limited variations (<0.5 °C) between 100 and 30 cm of snow depth, and a rapid decrease (>2 °C) below this value. Quantitatively, the dry runs reproduce the field values for permafrost locations, with a mismatch of less than 0.3 °C for snow depths of more than 10 cm. Below 10 cm, the mismatch exceeds 1.5 °C. Wet runs tend to underestimate the temperature of the permafrost-free areas by 0.2 to 0.5 °C. Yet above 20 cm of snow depth, the model results are compatible with the field values within 1σ for three of four subranges of snow depth. Below 20 cm of snow, the decrease in MAGST is more pronounced in the model output than in the field data and the underestimation by the model is close to 1 °C.

4.3. Sensitivity Test on the Water Balance

Figure 7 shows the sensitivity of the 1-m-deep and surficial mean annual ground temperature to the water balance (drainage/accumulation of water) for different snow depth (section 3.2.3). All MAT values are positively correlated with the March snow depth. For both surficial and 1-m-deep MAT and for all values of snow depth, the drained runs (negative external water flux leaving the soil column) exhibit colder mean annual temperatures than runs with a water inflow. For each curve, the evolution of the MAT with the external water flux is not linear, but consists of (i) a constant low value of the MAT until −2 mm/day; (ii) a transition from this low value to a higher value of the MAT between −2 and 1.5 mm/day, here called the drainage effect; and (iii) a plateau at this higher value, beyond 1.5 mm/day.

For MAT at the ground surface, the amplitude of the drainage effect is between 0.2 and 0.9 °C (Figure 7, right). It increases from 0 to 10 cm of snow depth before it decreases. Beyond 30 of snow depth, MAT remains more or less constant, so that values are similar for 30 and 100 cm of snow.

For MAT at 1-m depth (Figure 7, left), both the amplitude of the drainage effect and the absolute values of MATs increase with the snow depth. For snow-free conditions, the MAT evolves from −2.5 to −2.9 °C (0.4 °C difference), and for 30 cm of snow it increases from 0.8 to 2.8 °C (2 °C difference). For more than 30 cm of snow, the drainage effect does not become stronger and the absolute MAT values increase more slowly, so that the 100-cm snow depth curve evolves similarly to the 30-cm curve but with a global +0.4 °C

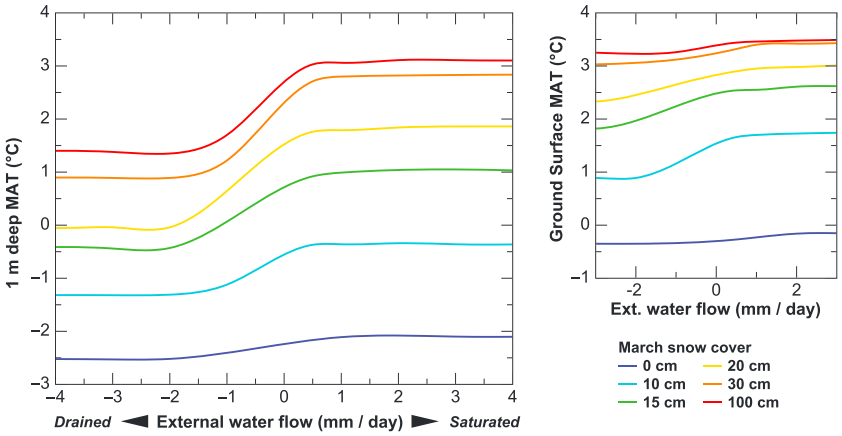

Figure 7. The 1-m-deep and surficial mean annual temperature dependence to drainage and snow depth as modeled with CryoGrid3. To evaluate the deep impact of drainage on the ground thermal regime, a spin-up of the 2015–2016 climate forcing was run until steady state was reached. Runs were performed for different snow depths and drainage conditions (see section 3.2.3). The upper surface of present-day stable permafrost is shallower than 1 m.

temperature shift. Together, the snow depth and the drainage condition create a 5.5 °C difference between the coldest and the warmest modeled 1-m-deep MAT.

5. Discussion

5.1. Field Measurements

The measured thaw depths are in good agreement with active layer thicknesses reported for Fennoscandian peat plateaus and palsas, with common depths around 50 cm (Christiansen et al., 2010; Sannel & Kuhry, 2011; Seppälä, 1976, 1990; Seppälä, 1983; Sjöberg et al., 2015). Our classification of stable and unstable permafrost sites is consistent with Åkerman and Johansson (2008), who report a temporal evolution of the active layers with stable active layers around 50 cm and deepening active layers between 60 and 100 cm. While our equipment did not allow to measure active layers deeper than 1 m, this study focuses on stable permafrost and permafrost-free sites, and both field measurements and modeling show active layer thickness of stable permafrost (in the steady state) to be less than 100 cm. This suggests that the measurements capture the active layer thickness of the stable permafrost. As mentioned before (section 3.1; thaw depths), the use of this “stable/instable permafrost” classification refers to the subsurface thermal regime and does not include the possible case where permafrost degradation occurs from the bottom, leading to subsidence without affecting the active layers.

The observed snow depths on peat plateaus and palsa tops are in the range of or slightly higher than those reported by Seppälä (1990) in Finnish Lapland (5 to 30 cm). A snow depth of 10 cm is also reported in Tabuchi and Seppälä (2012) on top of a smaller peat mound (60 cm high). On a peat plateau in northern Sweden, the mid-April snow depth varied between 0 and 25 cm between 2006 and 2013 (Sannel et al., 2016), with an increasing trend over the last four years. Furthermore, we confirm the observed difference in snow depths between plateaus and the surrounding wet mire, with on average 26-cm-higher snow depths in the mire. This difference in snow depths is a main driver for growth and stability of palsas (Seppälä, 1982, 1990, 1995, 2011), which is confirmed by MAGSTs (and FDDs) recorded for stable permafrost and permafrost-free locations. Our snow measurements illustrate the high variability of the snow depth also on peat plateaus, despite the generally low values. The plateau tops with stable permafrost can receive 80 or 100 cm of snow at localized spots, while there are locations with less than 20 cm of snow within the low-lying wet mires. These localized deviations from the main picture, most likely governed by wind drift patterns of snow, create stochasticity in the evolution of a plateau-palsa-mire area which might promote the initial formation of a palsa (Seppälä, 1982, 1995) or initiate the destabilization of a plateau.

Only sparse data are available to compare our distributed ground surface temperature time series for peat plateaus. Our MAGST values are warmer than those of Gisnås et al. (2014), where the same methodology

is applied to collect temperature time series for three sites with colder MAAT (2 °C difference): Svalbard, Jotunheimen, and low-alpine southern Norway (Finse). However, with a standard deviation (σ) of the 0.9 °C, the spatial variability in MAGST is in the same magnitude as the one reported by Gisnås et al. (2014) (σ between 0.7 and 1.3 °C). Yet both studies present 1-year-long data sets and the same observations over several years would make such comparison more robust. With a maximum difference of 3.4 °C between the coldest and the warmest MAGST and a 1.2 °C difference between the average temperature value of permafrost and permafrost-free locations, these results exemplify how the climate signal can be modulated in the ground and exhibit high variability at a metric to decametric scale. The same phenomenon is visible on Figure 5c, where highly different conditions are observed between a peat plateau and mire that are distant of 25 m. While the drier plateau site quickly freezes and reaches a minimum ground surface temperature −12 °C due to shallow winter snow depth and low water content (facilitating rapid autumn refreezing), the winter temperature is confined to 0 °C in the wet mire.

Measured FDD shows a systematic difference between permafrost and permafrost-free locations, with 89% of the permafrost-free locations recording FDDs of less than 200 °C.day while 67% of the stable permafrost location record FDDs exceeding 200 °C.day. As for the MAGST, this result is highly correlated to the snow depth (Figure 5c). Yet a significant variability remains, and for the same snow depth, measurements can yield a range of 200 to 400 °C.day, which suggests that additional factors impact the ground surface temperatures.

As this data set only covers one year, its representativeness is difficult to assess. In addition to the climate in the measurement period, transient effects might have an influence on the measured GSTs, such as the general ground thermal regime (in particular presence of permafrost) which is a result of longer-term climate (e.g., Riseborough, 2002). Therefore, measured GSTs might not only be determined by the climate forcing during the one-year study period, which could explain some of the mismatch between measured and modeled GST. In further investigations, transient studies spanning several decades should be conducted, but such is beyond the scope of the present study.

5.2. Model Results

Although the MAGSTs are positive (1.2–4.3 °C), the model successfully reproduces stable permafrost, in accordance with the field observations of thaw depth. Furthermore, Figure 6 shows that modifications of the water balance in CryoGrid3 by external inflow or outflow of water can reproduce the MAGST differences observed between permafrost and permafrost-free locations (i.e., peat plateaus and wet mires) for snow depths exceeding 20 cm. Below this value, the modeling results yield colder MAGST, with a mismatch higher than 1 °C. We interpret this mismatch to be a consequence of our model setup, which does not explicitly account for redistribution of snow, but instead scales snowfall with a snow threshold to reproduce measured March snow depths. Thus, in absence of significant melt or sublimation, the snow depth monotonically grows from November to March in the model, while wind-driven snow redistribution in reality creates a much more dynamic snow depth (Liston & Sturm, 1998). Peat plateaus and palsas for which 10 cm of snow were measured in March can potentially have experienced higher snow depths during prolonged periods, which were subsequently removed by wind drifting. Implementation of a blowing snow model (Lehning et al., 2006; Liston & Elder, 2006; Pomeroy et al., 1993) could help to resolve these problems.

Figure 6 confirms that the snow depth is not the only parameter modulating the thermal regime at the ground surface, what can partly explain the observed spread of FDDs for similar snow depth (Figure 5c). Consistent with previous work (Riseborough, 2002; Throop et al., 2012), the soil water content and drainage conditions affect ground surface temperatures, with well-drained sites systematically colder in both modeling and field measurements. While the model reliably reproduces MAGST for permafrost locations (and snow depths >20 cm), it underestimates MAGST for permafrost-free locations, so that the observed temperature difference between wet and dry conditions is underestimated by 0.2 to 0.5 °C. Also here, the most likely explanation for this underestimation is the lack of lateral snow redistribution between higher and lower locations in our model, which could cause a negative bias of snow depths especially in early winter (Figure S2 in the supporting information). Yet the model still shows a 0.5 °C difference between wet and dry runs which significantly affects the deeper thermal regime and the existence of permafrost (Figure 7). As this difference is even larger in the field measurements, we are confident that our conclusions on the role of the water balance and the drainage effect are conservative.

The saturation effect for wet runs and snow depth of more than 30 cm (Figure 7, red and orange curves) is in line with field measurements. Figure 5c exemplifies that a March snow depth of 35 cm is enough to prevent strong freezing of the ground for the wet mire site, maintaining a surface temperature of around 0 °C during the whole winter. Thicker snow depths produce the same effect, so that MAGST is maintained at a constant level.

Figure 7 demonstrates that drainage conditions have a major impact on ground temperatures. For high values of both drainage and inflow, the modeled MAT is not sensitive to the value of the external flux, as the active layer water content is at (or below) field capacity and at saturation, respectively. However, these two regimes feature MAT differences of up to 2 °C for the same climate forcing, which, together with the snow depth, determine the conditions for permafrost stability. For a typical winter snow depth of 15 to 20 cm, this drainage effect leads to permafrost conditions for well-drained ground situations, while permafrost cannot exist for saturated conditions (i.e., strong inflow of water).

As the microtopography of the peat plateaus determines both drainage conditions and snow depths, it has a distinct effect on their stability and evolution. As for other types of permafrost, the relative stability of peat plateaus is also related to their slow response time to changes on the climate forcing (Throop et al., 2012). On the one hand, plateaus that are high enough to both (i) have low winter snow depths and (ii) drain toward the surrounding mires benefit from favorable conditions for permafrost, even in a particularly warm year as 2015–2016, with some peat plateaus being in equilibrium with the climate of the last decades (Way et al., 2018). On the other hand, plateaus with higher winter snow depth are likely to subside progressively due to excess ice melt (Westermann et al., 2016), and eventually lose their ability to drain water to the surrounding wet mire, so that permafrost is no longer stable. Additional mechanisms are likely to interact with these effects depending on the vegetation cover. Jorgenson et al. (2010) showed that the vegetation succession could have an important negative feedback on the permafrost degradation, increasing its resilience to warming temperatures. Kurylyk et al. (2016) reported that, for forested peat plateaus, thaw-induced surface evolution modifies the surface albedo, resulting in another positive feedback on permafrost degradation. In addition, modeling experiments showed that palsas and peat plateaus could persist or quickly vanished depending on the chosen climate scenario (Way et al., 2018), highlighting the uncertainty of future climate projections as a decisive factor when modeling the fate of these permafrost features.

Sjöberg et al. (2016) showed the heat advection by groundwater flow could have a significant impact on the ground thermal regime. On the other hand, Kurylyk et al. (2016) reported that the mechanism was of limited importance in their studied configuration and suggested that it was highly dependent on the catchment and the pedologic/geologic subsurface material. Our modeling works do not include lateral groundwater flows and including this process likely represents an improvement of the description of the ground thermal regime. However, implementation in our 1-D model framework is not straightforward and would require information on lateral temperature gradients in the wet parts of the mire, as well as groundwater flow rates. However, as both of our study sites represent a rather flat topography, we consider it unlikely that heat advection by subsurface flow is a first-order control on the ground thermal regime which would create a significant bias in our conclusions.

The 3-D modeling experiments (Kurylyk et al., 2016) shown that lateral subsurface heat transfer have a significant impact on permafrost degradation. Due to the spatial distribution and geometry of elevated peat plateaus and low-lying wet mires (Figure 2), permafrost-underlain and permafrost-free features have extended contact margins, so that nonnegligible lateral heat fluxes can be expected. In the case of 1-D modeling these fluxes lead some author to overparameterize the geothermal heat fluxes to reproduce observed data (Way et al., 2018). For shallow water bodies surrounded by permafrost, Langer et al. (2016) showed that up to 70% of the heat induced by the water body was dissipated by lateral heat fluxes in this configuration. Therefore, a spatially distributed representation of microtopography and the resulting lateral heat and water fluxes holds significant potential to improve the model representation of peat plateaus. While such a scheme was presented in Aas et al. (2019), more work is needed to reproduce the thresholds of peat plateau stability and the dynamic response to climate change in models. In this study, we have presented a detailed observational data set, as well as one-dimensional modeling for the end-members of permafrost conditions, that is, stable permafrost and permafrost-free sites. Future studies should focus on how the microtopography

and geometry of peat plateau sites determines the spatial distribution of snow, as well as the lateral fluxes of water.

6. Conclusion

We present annual field data from two peat plateau sites in Northern Norway which, in conjunction with thermal modeling, facilitates assessing the environmental factors that govern the thermal stability of these permafrost features.

- Mean annual ground surface temperature of generally 2–2.5 °C is observed for stable permafrost locations, while permafrost-free locations mainly feature values between 3.5 and 4.5 °C.
- Freezing degree days are characterized by a noticeable threshold around 200 °C.day, which can largely separate permafrost and nonpermafrost locations.
- Simulating the ground thermal regime with CryoGrid3, we find that while snow has a critical importance on the winter thermal regime, this influence is strongly modulated by the water content of the soil at the surface and subsurface.
- We identify a drainage effect that can modify the 1-m-deep thermal regime of the soil by up to 2 °C between well-drained and water-saturated ground for the same snow depth, making it a decisive factor for the thermal stability of permafrost.
- The amplitude of this drainage effect is modulated by the snow depth and their interplay can create differences of up to 5 °C in mean annual ground temperatures at 1-m depth for the same climate forcing.

The "stable permafrost" classification refers to the subsurface thermal regime based on active layer measurements and does not include possible subsidence.

Acknowledgments
This work was funded by PERMANOR (Norwegian Research Council, KLIMAFORSK program, NFR project 255331), SatPERM (Norwegian Research Council, FRINATEK program, NFR project 239918) and the Department of Geosciences, University of Oslo, Norway. Ingvild Solheim is warmly thanked for the work of her master thesis and for her contribution to fieldwork. WRF simulations were performed on the Abel high-performance computing facility with resources provided by the Department of Geosciences of Oslo University. We thanks two anonymous reviewers for constructive feedbacks. The authors declare that they have no conflicts of interests. All data are available in the manuscript or the supporting information.

References

Aalto, J., Harrison, S., & Luoto, M. (2017). Statistical modelling predicts almost complete loss of major periglacial processes in northern Europe by. *Nature Communications*, *8*(1), 515–518. https://doi.org/10.1038/s41467-017-00669-3

Aalto, J., Venäläinen, A., Heikkinen, R. K., & Luoto, M. (2014). Potential for extreme loss in high-latitude Earth surface processes due to climate change. *Geophysical Research Letters*, *41*, 3914–3924. https://doi.org/10.1002/2014GL060095

Aas, K. S., Dunse, T., Collier, E., Schuler, T. V., Berntsen, T. K., Kohler, J., & Luks, B. (2016). The climatic mass balance of Svalbard glaciers: A 10-year simulation with a coupled atmosphere–glacier mass balance model. *The Cryosphere*, *10*(3), 1089–1104. https://doi.org/10.5194/tc-10-1089-2016

Aas, K. S., Martin, L., Nitzbon, J., Langer, M., Boike, J., Lee, H., et al. (2019). Thaw processes in ice-rich permafrost landscapes represented with laterally coupled tiles in a land surface model. *The Cryosphere*, *13*(2), 591–609. https://doi.org/10.5194/tc-13-591-2019

Åkerman, H. J., & Johansson, M. (2008). Thawing permafrost and thicker active layers in sub-arctic Sweden. *Permafrost and Periglacial Processes*, *19*(3), 279–292. https://doi.org/10.1002/ppp.626

Aune, B. (1993). Temperaturnormaler, normalperiode 1961–1990. *Norske Meteorological Institute Rapp Klima*, *1993*, 1–63.

Borge, A. F., Westermann, S., Solheim, I., & Etzelmüller, B. (2016). Strong degradation of palsas and peat plateaus in northern Norway during the last 60 years. *The Cryosphere Discussions*, 1–31. https://doi.org/10.5194/tc-2016-12

Chen, F., Mitchell, K., Schaake, J., Xue, Y., Pan, H.-L., Koren, V., et al. (1996). Modeling of land surface evaporation by four schemes and comparison with FIFE observations. *Journal of Geophysical Research-Atmospheres*, *101*(D3), 7251–7268. https://doi.org/10.1029/95JD02165

Christiansen, H. H., Etzelmüller, B., Isaksen, K., Juliussen, H., Farbrot, H., Humlum, O., et al. (2010). The thermal state of permafrost in the Nordic area during the international polar year 2007–2009. *Permafrost and Periglacial Processes*, *21*(2), 156–181. https://doi.org/10.1002/ppp.687

Ciais, P., Sabine, C., Bala, G., Bopp, L., Brovkin, V., & Canadell, J. (2013). Carbon and other biogeochemical cycles. In Intergovernmental Panel on Climate Change (Ed.), *Climate Change 2013—The Physical Science Basis* (pp. 465–570). Cambridge: Cambridge University Press. https://doi.org/10.1017/CBO9781107415324.015

Crichton, K. A., Bouttes, N., Roche, D. M., Chappellaz, J., & Krinner, G. (2016). Permafrost carbon as a missing link to explain CO_2 changes during the last deglaciation. *Nature Geoscience*, *9*(9), 683–686. https://doi.org/10.1038/ngeo2793

Dee, D. P., Uppala, S. M., Simmons, A. J., Berrisford, P., Poli, P., Kobayashi, S., et al. (2011). The ERA-Interim reanalysis: Configuration and performance of the data assimilation system. *Quarterly Journal of the Royal Meteorological Society*, *137*(656), 553–597. https://doi.org/10.1002/qj.828

Fronzek, S., Carter, T. R., Räisänen, J., Ruokolainen, L., & Luoto, M. (2010). Applying probabilistic projections of climate change with impact models: A case study for sub-arctic palsa mires in Fennoscandia. *Climatic Change*, *99*(3–4), 515–534. https://doi.org/10.1007/s10584-009-9679-y

Gisnås, K., Westermann, S., Schuler, T. V., Litherland, T., Isaksen, K., Boike, J., & Etzelmüller, B. (2014). A statistical approach to represent small-scale variability of permafrost temperatures due to snow cover. *The Cryosphere*, *8*(6), 2063–2074. https://doi.org/10.5194/tc-8-2063-2014

Grinde, L., Heiberg, H., Kristiansen, S., Mamen, J., Gangstø Skaland, R., Szewczyk-bartnicka, H., & Tilley Tajet, H. T. (2018). Været I Norge, Klimatologisk Oversikt, Året 2017. *MET info*. Oslo. Retrieved from https://www.met.no/publikasjoner/met-info/met-info-2017/_/attachment/download/06c46052-3343-4e67-9cb2-fa43ad4f0f46:1d260f20cc2299d9a2d196a3c5f6fe63e44abfaf/MET-info-13-2017.pdf

Heiberg, H., Kristiansen, S., Mamen, J., Gangstø Skaland, R., Szewczyk-Bartnicka, H., & Tilley Tajet, H. T. (2017). Været I Norge, Klimatologisk Oversikt, Året 2016. *MET info*. Oslo. Retrieved from https://www.met.no/publikasjoner/met-info/met-info-2016/_/attachment/download/c8e579ab-da7a-4e10-84c8-c7ed108ef47f:3a738a02dcc931e0e46a743a8bdc5fcab6fa8ed0/MET-info-13-2016.pdf

Jones, B. M., Baughman, C. A., Romanovsky, V. E., Parsekian, A. D., Babcock, E. L., Stephani, E., et al. (2016). Presence of rapidly degrading permafrost plateaus in south-central Alaska. *The Cryosphere*, *10*(6), 2673–2692. https://doi.org/10.5194/tc-10-2673-2016

Jorgenson, M. T., Romanovsky, V., Harden, J., Shur, Y., O'Donnell, J., Schuur, E. A. G., et al. (2010). Resilience and vulnerability of permafrost to climate change. This article is one of a selection of papers from the dynamics of change in Alaska's boreal forests: Resilience and vulnerability in response to climate warming. *Canadian Journal of Forest Research*, *40*(7), 1219–1236. https://doi.org/10.1139/X10-060

Kjellman, S. E., Axelsson, P. E., Etzelmüller, B., Westermann, S., & Sannel, A. B. K. (2018). Holocene development of subarctic permafrost peatlands in Finnmark, northern Norway. *The Holocene*, *28*(12), 1855–1869. https://doi.org/10.1177/0959683618798126

Köhler, P., Knorr, G., & Bard, E. (2014). Permafrost thawing as a possible source of abrupt carbon release at the onset of the Bølling/Allerød. *Nature Communications*, *5*(1), 5520. https://doi.org/10.1038/ncomms6520

Koven, C. D., Lawrence, D. M., & Riley, W. J. (2015). Permafrost carbon–climate feedback is sensitive to deep soil carbon decomposability but not deep soil nitrogen dynamics. *Proceedings of the National Academy of Sciences*, 201415123. https://doi.org/10.1073/pnas.1415123112

Koven, C. D., Riley, W. J., & Stern, A. (2013). Analysis of permafrost thermal dynamics and response to climate change in the CMIP5 Earth system models. *Journal of Climate*, *26*(6), 1877–1900. https://doi.org/10.1175/JCLI-D-12-00228.1

Koven, C. D., Ringeval, B., Friedlingstein, P., Ciais, P., Cadule, P., Khvorostyanov, D., et al. (2011). Permafrost carbon-climate feedbacks accelerate global warming. *Proceedings of the National Academy of Sciences*, *108*(36), 14,769–14,774. https://doi.org/10.1073/pnas.1103910108

Kremenetski, K., Velichko, A., Borisova, O., MacDonald, G., Smith, L., Frey, K., & Orlova, L. (2003). Peatlands of the Western Siberian lowlands: Current knowledge on zonation, carbon content and Late Quaternary history. *Quaternary Science Reviews*, *22*(5–7), 703–723. https://doi.org/10.1016/S0277-3791(02)00196-8

Kujala, K., Seppälä, M., & Holappa, T. (2008). Physical properties of peat and palsa formation. *Cold Regions Science and Technology*, *52*(3), 408–414. https://doi.org/10.1016/j.coldregions.2007.08.002

Kurylyk, B. L., Hayashi, M., Quinton, W. L., McKenzie, J. M., & Voss, C. I. (2016). Influence of vertical and lateral heat transfer on permafrost thaw, peatland landscape transition, and groundwater flow. *Water Resources Research*, *52*, 1286–1305. https://doi.org/10.1002/2015WR018057

Langer, M., Westermann, S., Boike, J., Kirillin, G., Grosse, G., Peng, S., & Krinner, G. (2016). Rapid degradation of permafrost underneath waterbodies in tundra landscapes-toward a representation of thermokarst in land surface models. *Journal of Geophysical Research: Earth Surface*, *121*, 2446–2470. https://doi.org/10.1002/2016JF003956

Lehning, M., Völksch, I., Gustafsson, D., Nguyen, T. A., Stähli, M., & Zappa, M. (2006). ALPINE3D: A detailed model of mountain surface processes and its application to snow hydrology. *Hydrological Processes*, *20*(10), 2111–2128. https://doi.org/10.1002/hyp.6204

Liljedahl, A. K., Boike, J., Daanen, R. P., Fedorov, A. N., Frost, G. V., Grosse, G., et al. (2016). Pan-Arctic ice-wedge degradation in warming permafrost and influence on tundra hydrology. *Nature Geoscience*, *9*(April), 312–318. https://doi.org/10.1038/ngeo2674

Liston, G. E., & Elder, K. (2006). A distributed snow-evolution modeling system (SnowModel). *Journal of Hydrometeorology*, *7*(6), 1259–1276. https://doi.org/10.1175/JHM548.1

Liston, G. E., & Sturm, M. (1998). A snow-transport model for complex terrain. *Journal of Glaciology*, *44*(148), 498–516. https://doi.org/10.3189/S0022143000002021

Luoto, M., Fronzek, S., & Zuidhoff, F. S. (2004). Spatial modelling of palsa mires in relation to climate in northern Europe. *Earth Surface Processes and Landforms*, *29*(11), 1373–1387. https://doi.org/10.1002/esp.1099

Mamet, S. D., Chun, K. P., Kershaw, G. G. L., Loranty, M. M., & Peter Kershaw, G. (2017). Recent increases in permafrost thaw rates and areal loss of palsas in the Western Northwest Territories, Canada. *Permafrost and Periglacial Processes*, *28*(4), 619–633. https://doi.org/10.1002/ppp.1951

McCalley, C. K., Woodcroft, B. J., Hodgkins, S. B., Wehr, R. A., Kim, E. H., Mondav, R., et al. (2014). Methane dynamics regulated by microbial community response to permafrost thaw. *Nature*, *514*(7523), 478–481. https://doi.org/10.1038/nature13798

Motorin, A. S., Bukin, A. V, & Iglovikov, A. V. (2017). Water-physical properties of drained peat soils of Northern Trans-Ural forest-steppe zone. *IOP Conference Series: Earth and Environmental Science*, 90, 012053. https://doi.org/10.1088/1755-1315/90/1/012053

Nitzbon, J., Langer, M., Westerman, S., Martin, L., Schanke Aas, K., & Boike, J. (2018). Modelling the degradation of ice-wedges in polygonal tundra under different hydrological conditions. *The Cryosphere Discussions*. https://doi.org/10.5194/tc-2018-211, 1–61.

Parviainen, M., & Luoto, M. (2007). Climate envelopes of mire complex types in Fennoscandia. *Geografiska Annaler. Series A, Physical Geography*, *89*(2), 137–151. https://doi.org/10.1111/j.1468-0459.2007.00314.x

Payette, S., Delwaide, A., Caccianiga, M., & Beauchemin, M. (2004). Accelerated thawing of subarctic peatland permafrost over the last 50 years. *Geophysical Research Letters*, *31*, L18208. https://doi.org/10.1029/2004GL020358

Pomeroy, J. W., Gray, D. M., & Landine, P. G. (1993). The Prairie Blowing Snow Model: Characteristics, validation, operation. *Journal of Hydrology*, *144*(1–4), 165–192. https://doi.org/10.1016/0022-1694(93)90171-5

Riseborough, D. W. (2002). The mean annual temperature at the top of permafrost, the TTOP model, and the effect of unfrozen water. *Permafrost and Periglacial Processes*, *13*(2), 137–143. https://doi.org/10.1002/ppp.418

Romanovsky, V. E., Drozdov, D. S., Oberman, N. G., Malkova, G. V., Kholodov, A. L., Marchenko, S. S., et al. (2010). Thermal state of permafrost in Russia. *Permafrost and Periglacial Processes*, *21*(2), 136–155. https://doi.org/10.1002/ppp.683

Romanovsky, V. E., & Osterkamp, T. E. (1995). Interannual variations of the thermal regime of the active layer and near-surface permafrost in northern Alaska. *Permafrost and Periglacial Processes*, *6*(4), 313–335. https://doi.org/10.1002/ppp.3430060404

Sannel, A. B. K., Hugelius, G., Jansson, P., & Kuhry, P. (2016). Permafrost warming in a subarctic peatland—Which meteorological controls are most important? *Permafrost and Periglacial Processes*, *27*(2), 177–188. https://doi.org/10.1002/ppp.1862

Sannel, A. B. K., & Kuhry, P. (2011). Warming-induced destabilization of peat plateau/thermokarst lake complexes. *Journal of Geophysical Research*, *116*, G03035. https://doi.org/10.1029/2010JG001635

Schuur, E. A. G., Abbott, B. W., Bowden, W. B., Brovkin, V., Camill, P., Canadell, J. G., et al. (2013). Expert assessment of vulnerability of permafrost carbon to climate change. *Climatic Change*, *119*(2), 359–374. https://doi.org/10.1007/s10584-013-0730-7

Schuur, E. A. G., Vogel, J. G., Crummer, K. G., Lee, H., Sickman, J. O., & Osterkamp, T. E. (2009). The effect of permafrost thaw on old carbon release and net carbon exchange from tundra. *Nature*, *459*(7246), 556–559. https://doi.org/10.1038/nature08031

Seppälä, M. (1972). The term "palsa.". *Zeitschrift für Geomorphologie*, *16*(4), 463.

Seppälä, M. (1976). Seasonal thawing of a palsa at Enontekiö Finnish Lapland in 1974. *Biuletyn Peryglacjalny*, *26*, 17–24.
Seppälä, M. (1982). An experimental study of the formation of palsas. *4th Canadian Permafrost Conference*, (September), 36–42.
Seppälä, M. (1983). Seasonal thawing of palsas in Finnish Lapland. In *Proceedings of the 4th international conference on permafrost* (pp. 18–22). Fairbanks, Alaska.
Seppälä, M. (1990). Depth of snow and Frost on a Palsa mire, Finnish Lapland. *Geografiska Annaler. Series A, Physical Geography*, *72*(2), 191. https://doi.org/10.2307/521114
Seppälä, M. (1995). How to make a palsa: A field experiment on permafrost formation. *Zeitschrift für Geomorphologie*, *99*, 91–96. https://doi.org/10.1127/zfgsuppl/99/1995/91
Seppälä, M. (2011). Synthesis of studies of palsa formation underlining the importance of local environmental and physical characteristics. *Quaternary Research*, *75*(02), 366–370. https://doi.org/10.1016/j.yqres.2010.09.007
Sherstyukov, A. B., & Sherstyukov, B. G. (2015). Spatial features and new trends in thermal conditions of soil and depth of its seasonal thawing in the permafrost zone. *Russian Meteorology and Hydrology*, *40*(2), 73–78. https://doi.org/10.3103/S1068373915020016
Shur, Y. L., & Jorgenson, M. T. (2007). Patterns of permafrost formation and degradation in relation to climate and ecosystems. *Permafrost and Periglacial Processes*, *18*(1), 7–19. https://doi.org/10.1002/ppp.582
Sjöberg, Y., Coon, E., Sannel, K., B, A., Pannetier, R., Harp, D., Frampton, A., et al. (2016). Thermal effects of groundwater flow through subarctic fens: A case study based on field observations and numerical modeling. *Water Resources Research*, *52*, 1591–1606. https://doi.org/10.1002/2015WR017571
Sjöberg, Y., Marklund, P., Pettersson, R., & Lyon, S. W. (2015). Geophysical mapping of palsa peatland permafrost. *The Cryosphere*, *9*(2), 465–478. https://doi.org/10.5194/tc-9-465-2015
Skamarock, W. C., & Klemp, J. B. (2008). A time-split nonhydrostatic atmospheric model for weather research and forecasting applications. *Journal of Computational Physics*, *227*(7), 3465–3485. https://doi.org/10.1016/j.jcp.2007.01.037
Sollid, J., & Sørbel, L. (1998). Palsa bogs as a climate indicator: Examples from Dovrefjell, southern Norway. *Research for Mountain Area Development: Europe*, *27*(4), 287–291. Retrieved from http://www.jstor.org/stable/4314737
Sollid, J. L., Andersen, S., Hamre, N., Kjeldsen, O., Salvigsen, O., Sturød, S., et al. (1973). Deglaciation of Finnmark, North Norway. *Norsk Geografisk Tidsskrift - Norwegian Journal of Geography*, *27*(4), 233–325. https://doi.org/10.1080/00291951.1973.9728306
Tabuchi, H., & Seppälä, M. (2012). Surface temperature inversion in the palsa and pounu fields of northern Finland. *Polar Science*, *6*(3–4), 237–251. https://doi.org/10.1016/j.polar.2012.10.001
Thibault, S., & Payette, S. (2009). Recent permafrost degradation in bogs of the James Bay area, northern Quebec, Canada. *Permafrost and Periglacial Processes*, *20*(4), 383–389. https://doi.org/10.1002/ppp.660
Throop, J., Lewkowicz, A. G., & Smith, S. L. (2012). Climate and ground temperature relations at sites across the continuous and discontinuous permafrost zones, northern Canada1. This article is one of a series of papers published in this CJES special issue on the theme of fundamental and applied research on. *Canadian Journal of Earth Sciences*, *49*(8), 865–876. https://doi.org/10.1139/e11-075
Walczak, R., & Rovdan, E. (2002). Water retention characteristics of peat and sand mixtures. *International Agrophysics*, *12*, 161–165.
Walter, K. M., Zimov, S. a., Chanton, J. P., Verbyla, D., & Chapin, F. S. (2006). Methane bubbling from Siberian thaw lakes as a positive feedback to climate warming. *Nature*, *443*(7107), 71–75. https://doi.org/10.1038/nature05040
Way, R. G., Lewkowicz, A. G., & Zhang, Y. (2018). Characteristics and fate of isolated permafrost patches in coastal Labrador, Canada. *The Cryosphere*, *12*(8), 2667–2688. https://doi.org/10.5194/tc-12-2667-2018
Westermann, S., Langer, M., Boike, J., Heikenfeld, M., Peter, M., Etzelmüller, B., & Krinner, G. (2016). Simulating the thermal regime and thaw processes of ice-rich permafrost ground with the land-surface model CryoGrid 3. *Geoscientific Model Development*, *9*(2), 523–546. https://doi.org/10.5194/gmd-9-523-2016
Westermann, S., Schuler, T. V., Gisnås, K., & Etzelmüller, B. (2013). Transient thermal modeling of permafrost conditions in southern Norway. *The Cryosphere*, *7*(2), 719–739. https://doi.org/10.5194/tc-7-719-2013
Zona, D. (2016). Long-term effects of permafrost thaw. *Nature*, *537*(7622), 625–626. https://doi.org/10.1038/537625a